ORIGINAL RESEARCH

Differential Phenotypes in Perivascular Adipose Tissue Surrounding the Internal Thoracic Artery and Diseased Coronary Artery

Ryosuke Numaguchi, MD;* Masato Furuhashi, MD, PhD;* Megumi Matsumoto, BSc; Hiroshi Sato, MD, PhD; Yosuke Yanase, MD, PhD; Yosuke Kuroda, MD, PhD; Ryo Harada, MD, PhD; Toshiro Ito, MD, PhD; Yukimura Higashiura, MD; Masayuki Koyama, MD, PhD; Marenao Tanaka, MD, PhD; Norihito Moniwa, MD, PhD; Masanori Nakamura, MD, PhD; Hirosato Doi, MD; Tetsuji Miura, MD, PhD; Nobuyoshi Kawaharada, MD, PhD

***Background*—**Perivascular adipose tissue (PVAT) is causally associated with vascular function and the pathogenesis of vascular disease in association with metabolically driven chronic inflammation called metaflammation. However, the difference in PVAT surrounding the coronary artery (CA-PVAT) and that surrounding the internal thoracic artery (ITA-PVAT), a vessel resistant to atherosclerosis, remains unclear. Herein, we investigated whether CA-PVAT, ITA-PVAT, and subcutaneous adipose tissue (SCAT) have distinct phenotypes.

***Methods and Results*—**Fat pads were sampled from 44 patients (men/women, 36:8; age, 67±13 years) with CA disease who underwent elective CA bypass grafting. Adipocyte size in ITA-PVAT and that in CA-PVAT were significantly smaller than that in SCAT. A greater extent of fibrosis and increased gene expression levels of fibrosis-related molecules were observed in CA-PVAT than those in SCAT and those in ITA-PVAT. CA-PVAT exhibited more pronounced metaflammation, as indicated by a significantly larger extent of CD68-positive and CD11c-positive M1 macrophages, a lower ratio of CD206-positive M2 to CD11c-positive M1 macrophages, a lower gene expression level of adiponectin, and higher gene expression levels of inflammatory cytokines and inflammasome- and endoplasmic reticulum stress–related molecules, than did ITA-PVAT and SCAT. Expression patterns of adipocyte developmental and pattern-forming genes were totally different among SCAT, ITA-PVAT, and CA-PVAT.

***Conclusions*—**The phenotype of ITA-PVAT is closer to that of SCAT than that of CA-PVAT, which may result from inherent differences in adipocytes. ITA-PVAT appears to be protected from metaflammation and consecutive adipose tissue remodeling, which may contribute to the decreased atherosclerotic plaque burden in the ITA. **(*J Am Heart Assoc*. 2019;8:e011147. DOI: 10.1161/JAHA.118.011147)**

Key Words: adipokine • adipose tissue • atherosclerosis • coronary artery bypass graft • fibrosis

Obesity is a risk factor for atherosclerotic cardiovascular disease.[1] Accumulation of visceral adipose tissue in obesity promotes a state of metabolically driven chronic and low-grade inflammation called metaflammation, which is characterized by abnormal adipokine production and activation of proinflammatory pathways.[2] Several bioactive molecules derived from adipose tissue, adipokines, have been implicated in the increased risk of atherosclerotic cardiovascular disease.[1,2] Adiponectin, a favorable adipokine, has been shown to modulate macrophage function in the direction of an anti-inflammatory phenotype.[3] Adiponectin directly increases insulin sensitivity and protects against initiation and progression of atherosclerosis. Conversely, induction of several chemokines and cytokines as adipokines and activation of inflammasomes and endoplasmic reticulum stress have been reported to be associated with obesity-induced insulin resistance and atherosclerosis.[1,2,4–6]

Adipose tissue in obesity is characterized by adipocyte hypertrophy, followed by immune cell infiltration, overproduction

From the Department of Cardiovascular Surgery (R.N., H.S., Y.Y., Y.K., R.H., T.I., H.D., N.K.), and Cardiovascular, Renal and Metabolic Medicine (M.F., M.M., Y.H., M.K., M.T., N.M., T.M.), Sapporo Medical University School of Medicine, Sapporo, Japan; Department of Cardiovascular Surgery, Sapporo City General Hospital, Sapporo, Japan (M.N.); and Department of Cardiovascular Surgery, Sapporo Cardiovascular Clinic, Sapporo, Japan (H.D.).

*Dr Numaguchi and Dr Furuhashi contributed equally to this work.

Correspondence to: Masato Furuhashi, MD, PhD, Department of Cardiovascular, Renal and Metabolic Medicine, Sapporo Medical University School of Medicine, S-1, W-16, Chuo-ku, Sapporo 060-8543, Japan. E-mail: furuhasi@sapmed.ac.jp

Received October 4, 2018; accepted December 12, 2018.

Clinical Perspective

What Is New?

- Augmented immune cell infiltration, induction of inflammatory cytokines, activation of inflammasomes and endoplasmic reticulum stress, and increased fibrosis were observed in perivascular adipose tissue (PVAT) surrounding the coronary artery compared with that surrounding the internal thoracic artery (ITA-PVAT) and subcutaneous adipose tissue of patients who underwent elective coronary artery bypass grafting surgery.
- Expression patterns of adipocyte developmental and pattern-forming genes were totally different among subcutaneous adipose tissue, ITA-PVAT, and PVAT surrounding the coronary artery.
- The phenotype of ITA-PVAT was closer to that of subcutaneous adipose tissue than that of PVAT surrounding the coronary artery, which may result from inherent differences in adipocytes.

What Are the Clinical Implications?

- Protection from metaflammation and consecutive adipose tissue remodeling in ITA-PVAT may contribute to the decreased atherosclerotic plaque burden in the ITA, an atherosclerosis-resistant vessel.

of extracellular matrix, and increased angiogenesis, a process that is referred to as adipose tissue remodeling.[7–9] Obesity induces infiltration of adipose tissue macrophages, which are characteristic of classically activated M1 macrophages, whereas resident macrophages in adipose tissue are alternatively activated M2 macrophages.[10] A shift to the activated M1-polarized state of adipose tissue macrophages from an M2-polarized state has been reported to contribute to metaflammation and insulin resistance.[10,11]

Perivascular adipose tissue (PVAT) has traditionally been thought to play a role in supporting vascular structure and metabolism. PVAT has recently been proposed to influence vascular function and the pathogenesis of vascular disease.[12] PVAT is implicated in the regulation of vascular tone by releasing adipose-derived relaxing and contracting factors, which contribute to the protection and progression of atherosclerotic vascular disease.[13–16] It has also been reported that chronic inflammation in the coronary adventitia and PVAT is associated with the pathogenesis of vasospastic angina.[17] Furthermore, epicardial fat may directly influence coronary atherogenesis and myocardial function because there is no fibrous fascial layer to impede diffusion of free fatty acids and adipokines from the fat underlying the myocardium and vessels.[18] It has been reported that epicardial adipose tissue is a source of inflammatory mediators.[19] Furthermore, an elevated volume of PVAT underlying the coronary artery (CA) was shown to be strongly associated with coronary atherosclerosis in combination with an imbalance of cytokines and adipokines.[20–22]

The internal thoracic artery (ITA) is protected from the development of atherosclerosis,[23] although the reasons are still largely unknown. The ITA is frequently used as the gold standard graft material for CA bypass grafting (CABG) because of its excellent long-term patency.[24] It has been reported that the ITA has less concentric atheromatous intimal thickening involving the whole circumference than does the right gastroepiploic artery, a candidate of graft vessels for CABG, even in patients with several coronary risk factors.[25] As another possible mechanism of the long-term patency of the ITA, excellent endothelial function, including shear stress sensing and generation of NO and antithrombotic factors, of the ITA has been reported to provide physiological and metabolic effects that are beneficial in both the graft and recipient CA.[23,24] However, the association of PVAT with vascular structure and function of the ITA and CA is not well understood. In the present study, we investigated the differential phenotype of fat pads on the structure and gene expression in PVAT surrounding the ITA (ITA-PVAT) and CA (CA-PVAT) in patients with CA disease who underwent elective CABG.

Methods

The data that support the findings of this study are available from the corresponding author on reasonable request.

Study Patients

Patients diagnosed with CA disease who underwent elective CABG surgery were recruited from Sapporo Medical University Hospital and the affiliated Sapporo Cardiovascular Clinic and Sapporo City General Hospital from May 2017 through March 2018. Patients treated with hemodialysis and those who underwent CABG without using the ITA were excluded. This study conformed to the principles outlined in the Declaration of Helsinki and was performed with the approval of the Ethical Committee of Sapporo Medical University. Written informed consent was received from all of the study subjects.

Collection of Fat Pads

Fat pads of subcutaneous adipose tissue (SCAT) from beneath the skin of the upper abdomen near the sternum, ITA-PVAT from the area of the left ITA, and CA-PVAT from the area of the left CA were collected during surgery before anticoagulation and establishment of extracorporeal circulation. The samples were divided into 2 parts. The first specimen was stored in formalin and embedded in paraffin for histological staining. The second specimen was frozen in liquid nitrogen for further mRNA isolation and real-time polymerase chain reaction.

Histological Analysis

Samples of fat pads were fixed in 10% formalin solution, dehydrated, and embedded in paraffin. Serial 5-μm sections were cut, mounted onto glass slides, deparaffinized, and rehydrated through degraded ethanol. Tissues were stained with hematoxylin-eosin and Masson's trichrome reagents.

Immunohistochemical staining using mouse anti-CD68 (Dako, Santa Clara, CA), rabbit anti-CD11c (Abcam, Cambridge, UK), also known as integrin α X chain, and mouse anti-CD206 (Abnova, Taipei, Taiwan), also known as mannose receptor C-type 1, antibodies was performed as previously described.[26,27] Control experiments were performed by omitting the primary antibodies.

Quantitative Image Analysis

Images were captured with a microscope (BIOREVO BZ-9000 with a BZ-II analyzer; Keyence, Osaka, Japan). Image analyses were performed using ImageJ and Fiji software. The cross-sectional area of an adipocyte in hematoxylin-eosin staining was determined by calculating the mean area of 200 randomly selected adipocytes per optical field at ×200 magnification. The results were averaged, and they are expressed as adipocyte size (μm^2). After checking sections of hematoxylin-eosin staining to avoid nonspecific fibrosis staining in the adventitia, sections were chosen to stain the fibrosis area in the inside, but not the edge, of adipose tissue from 19 consecutive patients, for whom sections in a set of 3 parts of adipose tissue were all adequate. Fibrosis was assessed on Masson's trichrome-stained tissue sections by quantifying the blue area representing collagen relative to the total tissue area at ×100 magnification. In 10 of the 19 patients, macrophage infiltration in tissue sections was assessed by quantifying the brown area stained by anti-CD68, anti-CD11c, or anti-CD206 antibodies relative to the total tissue area at ×100 magnification. For each quantitative analysis of fibrosis and macrophage infiltration, 3 randomly selected optical fields were examined per adipose tissue depot, and the results were averaged. Results are expressed as percentage positive area per total area. All of the measurements were performed in a double-blind manner by 2 different researchers (R.N., M.F.).

Quantitative Real-Time Polymerase Chain Reaction

Total RNA was isolated from samples in a set of 3 fat pads (n=27 each group) using the miRNeasy Micro Kit (Qiagen, Hilden, Germany). The amount and quality of isolated RNA were determined spectrophotometrically using Nanodrop (Thermo Fisher Scientific, Waltham, MA), and 500 ng of total RNA was reverse transcribed by using the high-capacity cDNA archive kit Reverse Transcription Kit (Applied Biosystems, Foster City, CA). Quantitative real-time polymerase chain reaction analysis was performed using SYBR Green in the real-time polymerase chain reaction system (Applied Biosystems, Warrington, UK). The thermal cycling program was 10 minutes at 95°C for enzyme activation and 40 cycles of denaturation for 15 s at 95°C, 30-s annealing at 58°C, and 30-s extension at 72°C. Primers used in the present study are listed in Table 1. To normalize expression data, 18s rRNA was used as an internal control gene.

Statistical Analysis

Numeric variables are expressed as mean±SD or mean±SEM for normal distributions or median (interquartile range) for skewed variables. Mixed model analysis was used for detecting significant differences in repeated measures data between SCAT, ITA-PVAT, and CA-PVAT. $P<0.05$ was considered statistically significant. All data were analyzed by using JMP for Macintosh (SAS Institute, Cary, NC).

Results

Basal Characteristics of the Studied Patients

Basal characteristics of the 44 recruited patients (men/women, 36:8) who underwent elective CABG surgery using the ITA are shown in Table 2. Age and body mass index of the recruited patients were 67±13 years and 24.4±4.1 kg/m^2, respectively. Most of the patients (95.5%) were diagnosed with multivessel CA disease. The numbers of patients with diabetes mellitus, hypertension, dyslipidemia, and myocardial infarction were 18 (40.9%), 31 (70.5%), 34 (77.3%), and 13 (29.5%), respectively. The ejection fraction assessed by echocardiography was 61±12%. Data for laboratory measurements are shown in Table 3.

Adipocyte Size in Fat Pads

Representative hematoxylin-eosin staining of SCAT, ITA-PVAT, and CA-PVAT is shown in Figure 1A. Adipocyte size in ITA-PVAT and that in CA-PVAT were significantly smaller than that in SCAT (Figure 1B). There was no significant difference in adipocyte size between ITA-PVAT and CA-PVAT. Crownlike structures, which have been reported to be composed of macrophages surrounding dead or dying adipocytes,[28] were observed in CA-PVAT but not in SCAT or ITA-PVAT.

Fibrosis in Fat Pads

Representative Masson's trichrome staining of SCAT, ITA-PVAT, and CA-PVAT is shown in Figure 2A. The fibrosis area in the inside, but not the edge, of adipose tissue in ITA-PVAT and

Table 1. Primers for Human Genes in Quantitative Real-Time PCR

Genes	Accession No.	Forward Primer	Reverse Primer
18s	M10098	5′-GTAACCCGTTGAACCCCATT-3′	5′-CCATCCAATCGGTAGTAGCG-3′
Adiponectin	NM_004797	5′-GGCATGACCAGGAAACCAC-3′	5′-TTCACCGATGTCTCCCTTAGG-3′
Asc	NM_145182	5′-TGGATGCTCTGTACGGGAAG-3′	5′-CCAGGCTGGTGTGAAACTGAA-3′
Cd163	NM_004244	5′-GCGGGAGAGTGGAAGTGAAAG-3′	5′-GTTACAAATCACAGAGACCGCT-3′
Cd206	NM_002438	5′-GGGTTGCTATCACTCTCTATGC-3′	5′-TTTCTTGTCTGTTGCCGTAGTT-3′
Chop	NM_004083	5′-GGAGAACCAGGAAACGGAAAC-3′	5′-TCTCCTTCATGCGCTGCTTT-3′
Col6a1	NM_001848	5′-ACAGTGACGAGGTGGAGATCA-3′	5′-GATAGCGCAGTCGGTGTAGG-3′
Emx2	NM_004098	5′-CGGCACTCAGCTACGCTAAC-3′	5′-CAAGTCCGGGTTGGAGTAGAC-3′
En1	NM_001426	5′-GAGCGCAGGGCACCAAATA-3′	5′-CGAGTCAGTTTTGACCACGG-3′
Grp78	NM_005347	5′-CATCACGCCGTCCTATGTCG-3′	5′-CGTCAAAGACCGTGTTCTCG-3′
Hoxa5	NM_019102	5′-AACTCATTTTGCGGTCGCTAT-3′	5′-TCCCTGAATTGCTCGCTCAC-3′
Il1b	NM_000576	5′-CACGATGCACCTGTACGATCA-3′	5′-GTTGCTCCATATCCTGTCCCT-3′
Il6	NM_000600	5′-AAATTCGGTACATCCTCGACGG-3′	5′-GGAAGGTTCAGGTTGTTTTCTGC-3′
Il10	NM_000572	5′-GACTTTAAGGGTTACCTGGGTTG-3′	5′-TCACATGCGCCTTGATGTCTG-3′
Mcp1	NM_002982	5′-CAGCCAGATGCAATCAATGCC-3′	5′-TGGAATCCTGAACCCACTTCT-3′
Mincle	NM_014358	5′-CTGAAACACAATGCACAGAGAGA-3′	5′-AAAGATGCGAAATGTCACAACAC-3′
Nlrp3	NM_001127462	5′-GATCTTCGCTGCGATCAACAG-3′	5′-CGTGCATTATCTGAACCCCAC-3′
Pdgfb	NM_033016.2	5′-CTCGATCCGCTCCTTTGATGA-3′	5′-CGTTGGTGCGGTCTATGAG-3′
Tgfb	NM_000660	5′-CAAGCAGAGTACACACAGCAT-3′	5′-TGCTCCACTTTTAACTTGAGCC-3′
Timp1	NM_003254	5′-CTTCTGCAATTCCGACCTCGT-3′	5′-ACGCTGGTATAAGGTGGTCTG-3′
Tnfa	NM_000594	5′-GAGGCCAAGCCCTGGTATG-3′	5′-CGGGCCGATTGATCTCAGC-3′

PCR indicates polymerase chain reaction.

that in CA-PVAT were significantly larger than that in SCAT (Figure 2B). CA-PVAT had a significantly larger fibrosis area than did ITA-PVAT (Figure 2B). ITA-PVAT and CA-PVAT had significantly higher gene expressions of fibrosis-related molecules, transforming growth factor-β, and macrophage-inducible C-type lectin (MINCLE), also known as C-type lectin domain family 4 member E, than did SCAT; and gene expression levels of transforming growth factor-β and MINCLE in CA-PVAT were significantly higher than those in ITA-PVAT (Figure 2C). Gene expression levels of other fibrosis-related molecules, including tissue inhibitor of metalloproteinase 1, platelet-derived growth factor subunit B, and collagen type 6 α 1 chain, in CA-PVAT were significantly higher than those in SCAT and those in ITA-PVAT (Figure 2C).

Macrophage Infiltration in Fat Pads

Representative immunohistological staining, including CD68, a marker of macrophages, CD11c, a marker of M1 macrophages, and CD206, a marker of M2 macrophages, of SCAT, ITA-PVAT, and CA-PVAT is shown in Figure 3A. The macrophage infiltration area stained by anti-CD68 antibody in ITA-PVAT and that in CA-PVAT were significantly larger than that in SCAT (Figure 3B). The inflammatory area of M1 phenotype of macrophage infiltration stained by anti-CD11c antibody in CA-PVAT was significantly larger than that in SCAT and that in ITA-PVAT (Figure 3C). The area of M2 phenotype of macrophage infiltration stained by anti-CD206 antibody in ITA-PVAT and that in CA-PVAT were significantly larger than that in SCAT (Figure 3D). The ratio of CD206-positive to CD11c-positive macrophages in CA-PVAT was significantly lower than that in SCAT and that in ITA-PVAT (Figure 3E).

Metaflammation in Fat Pads

Gene expression levels of monocyte chemoattractant protein-1, a chemokine, and inflammatory cytokines, including interleukin-1β, interleukin-6, and tumor necrosis factor-α, in CA-PVAT were significantly higher than those in SCAT and those in ITA-PVAT (Figure 4A). Gene expression levels of M2 macrophage markers, CD163 and CD206, in ITA-PVAT and those in CA-PVAT were significantly higher than those in SCAT (Figure 4B). The gene expression level of interleukin-10, an anti-inflammatory cytokine as an M2 macrophage-related marker, in ITA-PVAT, but not that in CA-PVAT, was significantly higher than that in SCAT (Figure 4B).

Table 2. Characteristics of the Recruited Patients

Characteristics	Value
No. (men/women)	44 (36:8)
Age, y	67±13
Body mass index, kg/m^2	24.4±4.1
Systolic blood pressure, mm Hg	125±15
Diastolic blood pressure, mm Hg	72±14
Pulse rate, bpm	74±15
Coronary artery disease	
1-Vessel disease	2 (4.5)
2-Vessel disease	13 (29.5)
3-Vessel disease	29 (65.9)
Complications	
Diabetes mellitus	18 (40.9)
Hypertension	31 (70.5)
Dyslipidemia	34 (77.3)
Myocardial infarction	13 (29.5)
Medications	
Oral antidiabetic drugs	11 (25.0)
Insulin	5 (11.4)
ACEI or ARB	19 (43.2)
β Blocker	20 (45.5)
Statin	31 (70.5)
Antiplatelet drugs	38 (86.4)
Echocardiography	
Ejection fraction, %	61±12

Variables are expressed as number (percentage) or mean±SD. ACEI indicates angiotensin-converting enzyme inhibitor; ARB, angiotensin receptor blocker; bpm, beats per minute.

Table 3. Laboratory Measurements

Variable	Value
Hemoglobin, g/dL	12.8±2.0
AST, IU/L	28 (22–36)
ALT, IU/L	23 (16–38)
γGTP, IU/L	27 (20–44)
Blood urea nitrogen, mg/dL	17 (13–22)
Creatinine, mg/dL	0.91 (0.79–1.07)
eGFR, mL/min per 1.73 m^2	62.0±16.9
Uric acid, g/dL	6.2±1.4
Total cholesterol, mg/dL	159±38
LDL cholesterol, mg/dL	88±35
HDL cholesterol, mg/dL	47±11
Triglycerides, mg/dL	115 (71–137)
Fasting glucose, mg/dL	100 (90–117)
Insulin, μU/mL	2.3 (1.0–5.5)
HOMA-R	0.54 (0.28–1.34)
HbA1c, %	6.1±0.9
NT-proBNP, pg/mL	162 (40–277)

Variables are expressed as mean±SD or median (interquartile range). ALT indicates alanine transaminase; AST, aspartate transaminase; eGFR, estimated glomerular filtration rate; γGTP, γ-glutamyl transpeptidase; HbA1c, hemoglobin A1c; HDL, high-density lipoprotein; HOMA-R, homeostasis model assessment of insulin resistance; LDL, low-density lipoprotein; NT-proBNP, N-terminal pro-B-type natriuretic peptide.

The gene expression level of adiponectin, an adipokine with antiatherogenic and anti-inflammatory features, in CA-PVAT was significantly lower than that in SCAT and that in ITA-PVAT (Figure 4C), whereas gene expression levels of inflammasome-related molecules, including nucleotide-binding domain, leucine-rich–containing family, pyrin domain–containing-3 and apoptosis-associated specklike protein containing caspase recruitment domain, and endoplasmic reticulum stress-related molecules, including glucose-regulated protein 78 and C/EBP homologous protein, in CA-PVAT were significantly higher than those in SCAT and those in ITA-PVAT (Figure 4C).

Adipocyte Developmental and Pattern-Forming Genes in Fat Pads

To address phenotypic differences in 3 parts of adipose tissue, gene expression levels of adipocyte developmental and pattern-forming genes, as previously indicated,[29–31] including engrailed homeobox 1, empty spiracles homeobox 2, and homeobox A5, were investigated (Figure 4D). ITA-PVAT had significantly lower gene expression levels of engrailed homeobox 1 and empty spiracles homeobox 2 and higher gene expression level of homeobox A5 than did SCAT, whereas CA-PVAT had a significantly lower gene expression level of engrailed homeobox 1 than did SCAT. Expression patterns of these developmental and pattern-forming genes were totally different among SCAT, ITA-PVAT, and CA-PVAT.

Discussion

The present study demonstrated pronounced metaflammation and consecutive adipose tissue remodeling (namely, augmented immune cell infiltration, induction of inflammatory cytokines, activation of inflammasomes and endoplasmic reticulum stress, and increased fibrosis) in CA-PVAT compared with those in ITA-PVAT and SCAT of patients who underwent elective CABG surgery. The phenotypic difference of metaflammation in CA-PVAT might be linked to susceptibility of the CA surrounded by epicardial fat to atherosclerosis. The phenotype of ITA-PVAT was closer to that of SCAT than that of CA-PVAT. Protection from metaflammation in ITA-

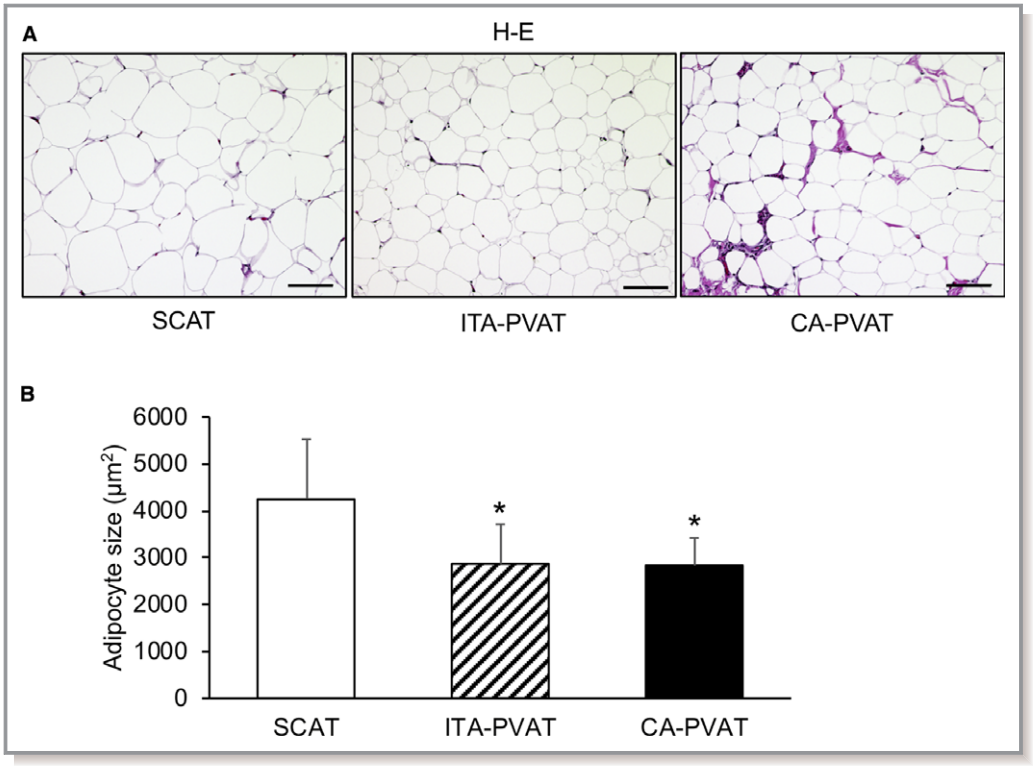

Figure 1. Adipocyte size in fat pads. **A**, Representative hematoxylin-eosin (H-E) staining of subcutaneous adipose tissue (SCAT) and of perivascular adipose tissue surrounding the internal thoracic artery (ITA-PVAT) and that surrounding the coronary artery (CA-PVAT). Bar=100 μm. **B**, Comparison of adipocyte sizes in SCAT, ITA-PVAT, and CA-PVAT (n=44 in each group). Results are shown as mean±SD. **P*<0.05 vs SCAT.

PVAT may contribute to the decreased atherosclerotic plaque burden in the ITA. Furthermore, a differential expression pattern of adipocyte developmental and pattern-forming genes, as previously indicated,[29–31] was observed in distinct adipose tissue, suggesting that fat depot–specific features result from inherent differences in adipocytes. To the best of our knowledge, this is the first study in which the differential phenotype of metaflammation in fat pads surrounding the ITA, an atherosclerosis-resistant vessel, was investigated in comparison to that surrounding the CA.

Epicardial fat shares a common embryological origin with mesenteric and omental fat, and the origin is the splanchnopleuric mesoderm associated with the gut.[32] Anatomically separated regional adipose depots have also been shown to be distinct with respect to gene expression patterns and functional characteristics.[29–31] It has been reported that in vitro differentiation of preadipocytes isolated from regional adipose depots produces adipocytes that phenotypically resemble in vivo counterparts of adipocytes.[29–31,33] Phenotypic differences in adipocytes can stem from developmental divergence of precursor cells in distinct adipose tissue. In the present study, the expression patterns of adipocyte developmental and pattern-forming genes, as previously indicated,[29–31] including engrailed homeobox 1, empty spiracles homeobox 2, and homeobox A5, were totally different among SCAT, ITA-PVAT, and CA-PVAT. Fat pads from ITA-PVAT and CA-PVAT exhibited unique gene expression profiles that underlie their roles in vascular homeostasis. These findings are consistent with the notion that adipocytes residing in these depots are derived from distinct precursor cells, which may underlie the phenotypic differences, although immune cells in adipose tissue may have some effects.

The ITA arises from the subclavian artery and exists in a stable retrosternal position. On the other hand, the CA kinks and twists on every heartbeat, and the internal lamina of the CA is constantly experiencing tissue friction and exhaustion, which subsequently allows the migration of cells and infiltration of plasma contents, resulting in accelerated progression of atherosclerosis of the artery, particularly in patients with hyperlipidemia and/or diabetes mellitus.[34,35] Mechanical stress as well as metabolic stress may cause genetic and epigenetic changes of several inflammatory genes, leading to more pronounced metaflammation in CA-PVAT compared with that in ITA-PVAT, especially in patients complicated with metabolic diseases, including obesity, diabetes mellitus, dyslipidemia, and hypertension.

Segments of coronary arteries lacking epicardial fat or separated from epicardial fat by a bridge of myocardial tissue have been reported to be protected against the development of atherosclerosis.[36,37] On the other hand, the development of PVAT

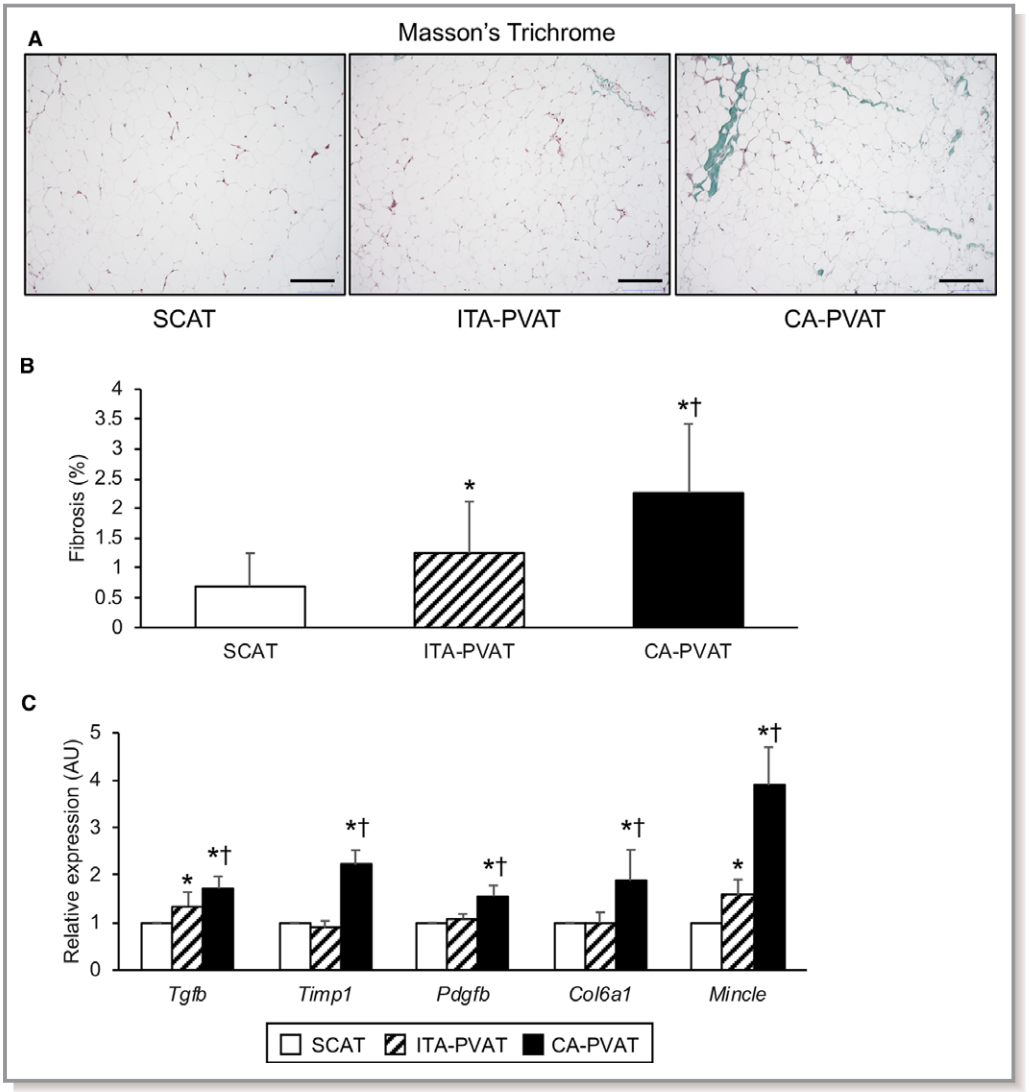

Figure 2. Fibrosis in fat pads. **A**, Representative Masson's trichrome staining of subcutaneous adipose tissue (SCAT) and of perivascular adipose tissue surrounding the internal thoracic artery (ITA-PVAT) and that surrounding the coronary artery (CA-PVAT). Bar=200 μm. **B**, Fibrosis areas in SCAT, ITA-PVAT, and CA-PVAT (n=19 in each group). Results are shown as mean±SD. **C**, Gene expression levels of fibrosis-related molecules, including transforming growth factor-β (TGF-β), tissue inhibitor of metalloproteinase 1 (TIMP1), platelet-derived growth factor subunit B (PDGFB), collagen type 6 α 1 chain (COL6a1), and macrophage-inducible C-type lectin (MINCLE), in SCAT, ITA-PVAT, and CA-PVAT (n=27 in each group). Results are shown as relative expression of each target gene in SCAT of each patient and as mean±SEM. AU indicates arbitrary unit. **P*<0.05 vs SCAT; †*P*<0.05 vs ITA-PVAT.

has been reported to be reduced and impaired with increased inflammation in the experimental models of atherosclerosis,[38,39] suggesting that the lack of normal PVAT is sufficient to drive increased atherosclerosis. Autopsy analyses demonstrated that there was more macrophage infiltration in epicardial fat in vessels with large necrotic core plaques than in vessels without lipid core plaques.[18,40] It has also been reported that artery tertiary lymphoid organs in the adventitial connective tissue surrounding arteries control atherosclerosis immune responses and protect against atherosclerosis via vascular smooth muscle cell lymphotoxin β receptor signaling.[41] In the present study, patients without CA disease were not included as a control group. Therefore, it is difficult to determine whether the inflammatory response in PVAT is the cause or the result of atherosclerosis. Mechanistic studies are needed to clarify what underlies the relationship between the development of atherosclerosis and differential phenotypes of PVAT. In addition, the association of ITA-PVAT with other factors that may affect resistance of the ITA to atherosclerosis, including shear stress,[23,24] endothelium-dependent vasodilatation,[24,42] and the difference in gene expression levels of proatherogenic and antiatherogenic proteins in endothelial cells,[43,44] also needs to be clarified.

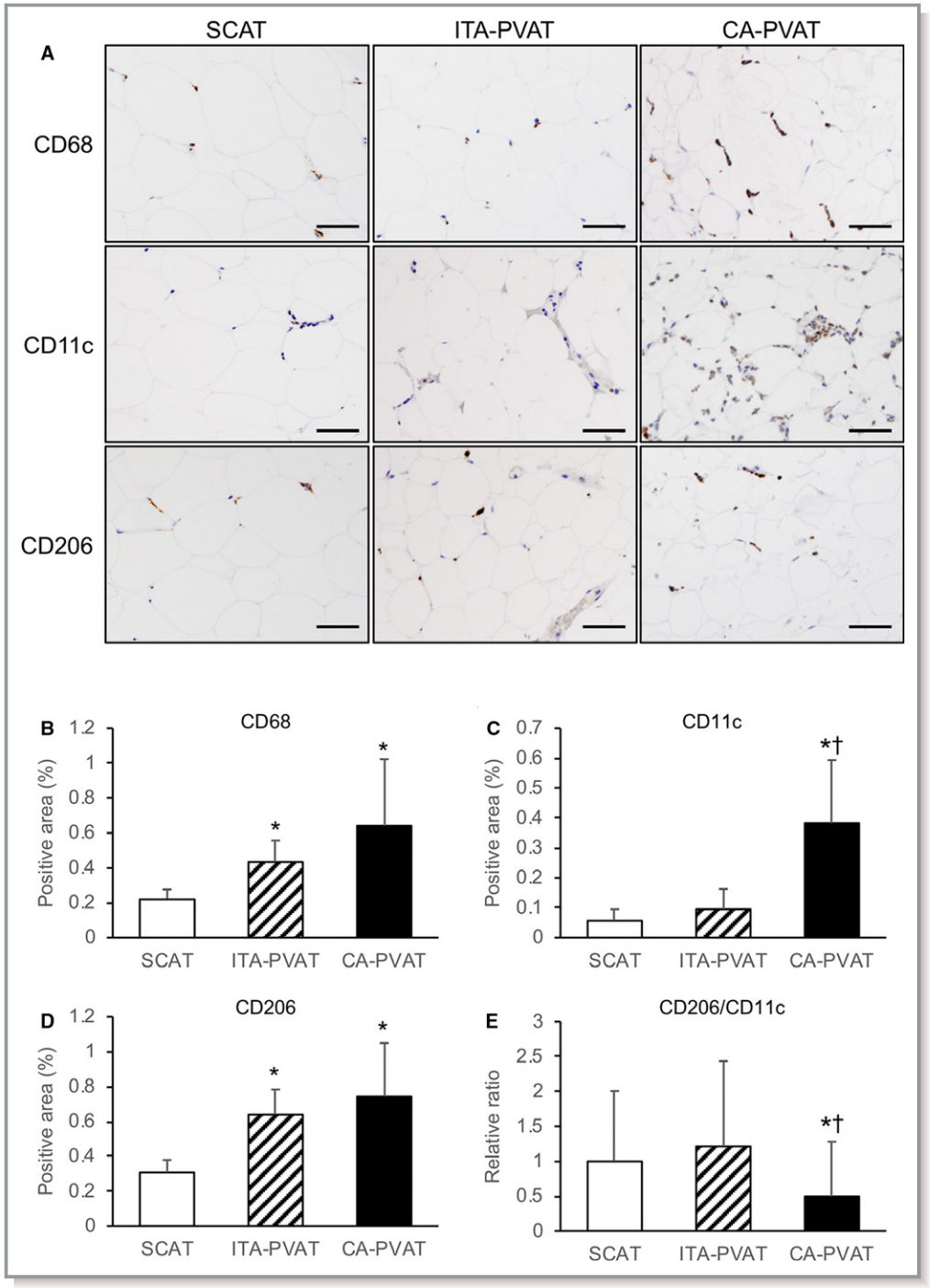

Figure 3. Macrophage infiltration in fat pads. **A**, Representative immunohistological staining, including CD68 (a marker of macrophages), CD11c (a marker of M1 macrophages), and CD206 (a marker of M2 macrophages), of subcutaneous adipose tissue (SCAT) and of perivascular adipose tissue surrounding the internal thoracic artery (ITA-PVAT) and that surrounding the coronary artery (CA-PVAT). Bar=50 μm. **B** through **D**, Positive areas of immunohistological staining of CD68, CD11c, and CD206 in SCAT, ITA-PVAT, and CA-PVAT (n=10 in each group). **E**, Ratios of the macrophage infiltration areas of CD206 to CD11c in SCAT, ITA-PVAT, and CA-PVAT. Results are shown as mean±SD. **P*<0.05 vs SCAT; †*P*<0.05 vs ITA-PVAT.

Adipose tissue fibrosis is thought to limit the expandability of adipose tissue during the development of obesity, leading to ectopic fat accumulation in nonadipose tissue, such as the liver and skeletal muscle.[8,9,45] In fact, adipose tissue fibrosis has been reported to be negatively correlated with adipocyte size in human adipose tissue.[46] It has recently been reported that MINCLE is mainly localized to proinflammatory M1 macrophages in crownlike structures of adipose tissue[47] and

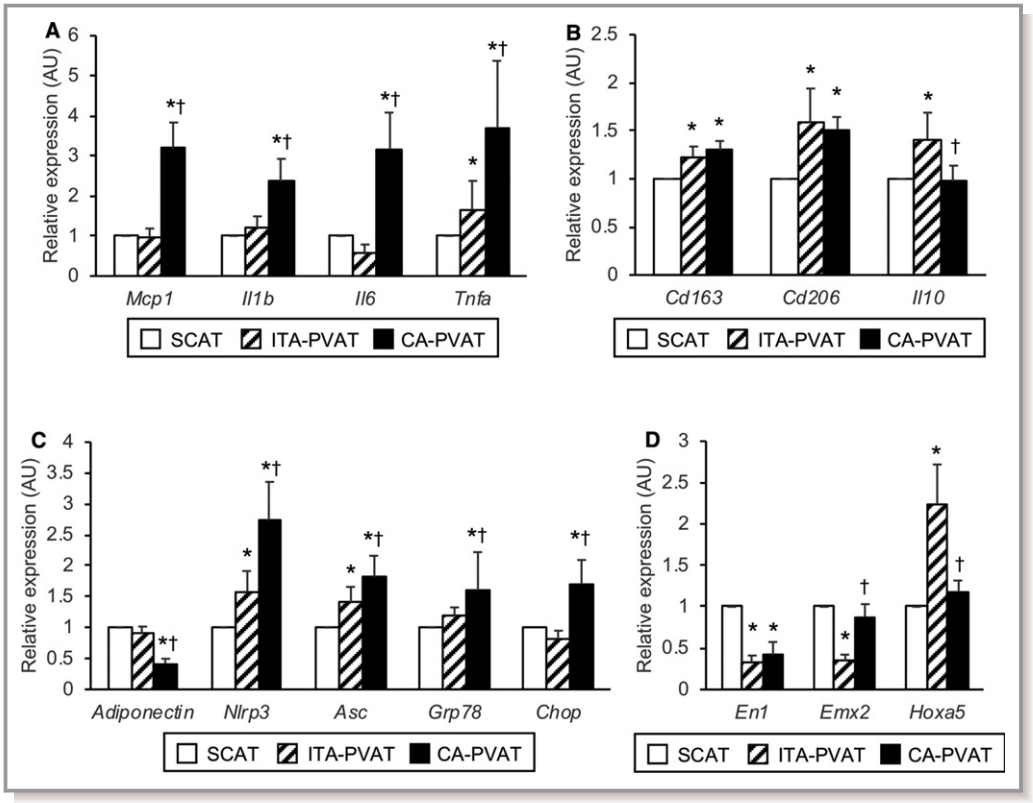

Figure 4. Metaflammation and adipocyte developmental and pattern-forming factors in fat pads. **A**, Gene expression levels of inflammatory molecules, including monocyte chemoattractant protein-1 (MCP-1), interleukin-1β (IL-1β), interleukin-6 (IL-6), and tumor necrosis factor-α (TNFα), in subcutaneous adipose tissue (SCAT) and in perivascular adipose tissue surrounding the internal thoracic artery (ITA-PVAT) and that surrounding the coronary artery (CA-PVAT). **B**, Gene expression levels of M2-polarized state-related molecules, including CD163, CD206, and interleukin-10 (IL-10), in SCAT, ITA-PVAT, and CA-PVAT. **C**, Gene expression levels of adiponectin, inflammasome-related molecules, including nucleotide-binding domain, leucine-rich–containing family, pyrin domain–containing-3 (NLRP3) and apoptosis-associated specklike protein containing caspase recruitment domain (ASC), and endoplasmic reticulum stress-related molecules, including glucose-regulated protein 78 (GRP78) and C/EBP homologous protein (CHOP), in SCAT, ITA-PVAT, and CA-PVAT. **D**, Gene expression levels of adipocyte developmental and pattern-forming factors, including engrailed homeobox 1 (EN1), empty spiracles homeobox 2 (EMX2), and homeobox A5 (HOXA5), in SCAT, ITA-PVAT, and CA-PVAT (n=27 in each group). Results are shown as relative expression of each target gene in SCAT of each patient and as mean±SEM. AU indicates arbitrary unit. *P<0.05 vs SCAT; †P<0.05 vs ITA-PVAT.

that it promotes the development of interstitial fibrosis.[48] In the present study, ITA-PVAT and CA-PVAT had significantly greater extents of fibrosis with higher gene expression level of MINCLE and smaller adipocyte size than did SCAT. As previously reported,[9] healthy adipose tissue expansion, which is achieved in an anti-inflammatory state through enlargement of preexisting adipocytes by lipid accumulation as adipocyte hypertrophy, may occur in SCAT, whereas CA-PVAT and ITA-PVAT harbor unhealthy pathological adipose tissue expansion with fibrosis, which may result from higher gene expression levels of metaflammation-related molecules, including MINCLE. Similar to our results, it was previously reported that a greater extent of fibrosis was observed in CA-PVAT than in ITA-PVAT.[49]

Intravascular and organ infections were critical in the preantibiotic era, and the presence of PVAT may have been beneficial by ensuring a strong macrophage immune response or by maintaining adipose tissue energy stores as part of the thirfty phenotype to survive. Proinflammatory properties of epicardial fat, including CA-PVAT, which is involved in cardiovascular systems, especially the heart pumping blood to organs, may have been crucial in controlling such infections in the remote past. It has been reported that a short-term high-fat diet upregulated proinflammatory gene expression in PVAT of mice, suggesting that dietary lipids may be analogous to bacterial membrane lipids, such as endotoxins, and activate innate immune signaling pathways that lead to enhanced vascular inflammation.[31,50] It has also been reported that

metaflammation in adipose tissue promotes an angiogenic response.[50,51] As another potential significance of increased metaflammation in CA-PVAT, inflammatory reaction derived from CA-PVAT could be beneficial by the development of collateral circulation in patients with obstructive CA disease.

This study has several limitations. First, the number of patients was small, and there would have been selection bias of patients. Second, because the recruited patients were only Japanese people, it is unclear whether the present findings can be generalized to other ethnicities. Third, because this study was a cross-sectional study using patients with CA disease, the study does not prove a causal relationship between inflammatory changes in adipose tissue and the development and progression of atherosclerosis. Finally, the recruited patients had several diseases, including diabetes mellitus, hypertension, and dyslipidemia, and had been treated with several drugs, including angiotensin-converting enzyme inhibitors, angiotensin receptor blockers, and statins. At the basal point, mean body mass index was <25 kg/m^2, and mean systolic and diastolic blood pressures were within normal ranges. Lifestyle-related diseases and administration of drugs may have affected the extent of metaflammation and fibrosis in adipose tissue.

In conclusion, the phenotype of ITA-PVAT is closer to that of SCAT than that of CA-PVAT. The differential expression pattern of adipocyte developmental and pattern-forming genes in distinct adipose tissue may be a potential mechanism underlying the difference in metaflammation in distinct adipose tissue. CA-PVAT had a significantly larger extent of CD11c-positive M1 macrophages, a lower ratio of CD206-positive M2 to CD11c-positive M1 macrophages, higher gene expression levels of several inflammatory cytokines, lower gene expression levels of anti-inflammatory adipokines, more activation of inflammasomes and endoplasmic reticulum stress, and increased fibrosis than did ITA-PVAT and SCAT. ITA-PVAT appears to be protected from pronounced metaflammation and consecutive adipose tissue remodeling, which may contribute to the decreased atherosclerotic plaque burden in the ITA, an atherosclerosis-resistant vessel.

Sources of Funding

Furuhashi has been supported by a grant from Japan Society for the Promotion of Science (JSPS)-KAKENHI.

Disclosures

None.

References

1. Gregor MF, Hotamisligil GS. Inflammatory mechanisms in obesity. *Annu Rev Immunol*. 2011;29:415–445.
2. Hotamisligil GS. Inflammation, metaflammation and immunometabolic disorders. *Nature*. 2017;542:177–185.
3. Kadowaki T, Yamauchi T, Kubota N, Hara K, Ueki K, Tobe K. Adiponectin and adiponectin receptors in insulin resistance, diabetes, and the metabolic syndrome. *J Clin Invest*. 2006;116:1784–1792.
4. Wen H, Ting JP, O'Neill LA. A role for the NLRP3 inflammasome in metabolic diseases—did warburg miss inflammation? *Nat Immunol*. 2012;13:352–357.
5. Karasawa T, Takahashi M. Role of NLRP3 inflammasomes in atherosclerosis. *J Atheroscler Thromb*. 2017;24:443–451.
6. Hotamisligil GS. Endoplasmic reticulum stress and the inflammatory basis of metabolic disease. *Cell*. 2010;140:900–917.
7. Halberg N, Khan T, Trujillo ME, Wernstedt-Asterholm I, Attie AD, Sherwani S, Wang ZV, Landskroner-Eiger S, Dineen S, Magalang UJ, Brekken RA, Scherer PE. Hypoxia-inducible factor 1alpha induces fibrosis and insulin resistance in white adipose tissue. *Mol Cell Biol*. 2009;29:4467–4483.
8. Sun K, Kusminski CM, Scherer PE. Adipose tissue remodeling and obesity. *J Clin Invest*. 2011;121:2094–2101.
9. Kusminski CM, Bickel PE, Scherer PE. Targeting adipose tissue in the treatment of obesity-associated diabetes. *Nat Rev Drug Discov*. 2016;15:639–660.
10. Lumeng CN, Bodzin JL, Saltiel AR. Obesity induces a phenotypic switch in adipose tissue macrophage polarization. *J Clin Invest*. 2007;117:175–184.
11. Wentworth JM, Naselli G, Brown WA, Doyle L, Phipson B, Smyth GK, Wabitsch M, O'Brien PE, Harrison LC. Pro-inflammatory CD11C+CD206+ adipose tissue macrophages are associated with insulin resistance in human obesity. *Diabetes*. 2010;59:1648–1656.
12. Szasz T, Webb RC. Perivascular adipose tissue: more than just structural support. *Clin Sci (Lond)*. 2012;122:1–12.
13. Mendizabal Y, Llorens S, Nava E. Vasoactive effects of prostaglandins from the perivascular fat of mesenteric resistance arteries in WKY and SHROB rats. *Life Sci*. 2013;93:1023–1032.
14. Meyer MR, Fredette NC, Barton M, Prossnitz ER. Regulation of vascular smooth muscle tone by adipose-derived contracting factor. *PLoS One*. 2013;8:e79245.
15. Owen MK, Witzmann FA, McKenney ML, Lai X, Berwick ZC, Moberly SP, Alloosh M, Sturek M, Tune JD. Perivascular adipose tissue potentiates contraction of coronary vascular smooth muscle: influence of obesity. *Circulation*. 2013;128:9–18.
16. Saxton SN, Ryding KE, Aldous RG, Withers SB, Ohanian J, Heagerty AM. Role of sympathetic nerves and adipocyte catecholamine uptake in the vasorelaxant function of perivascular adipose tissue. *Arterioscler Thromb Vasc Biol*. 2018;38:880–891.
17. Ohyama K, Matsumoto Y, Takanami K, Ota H, Nishimiya K, Sugisawa J, Tsuchiya S, Amamizu H, Uzuka H, Suda A, Shindo T, Kikuchi Y, Hao K, Tsuburaya R, Takahashi J, Miyata S, Sakata Y, Takase K, Shimokawa H. Coronary adventitial and perivascular adipose tissue inflammation in patients with vasospastic angina. *J Am Coll Cardiol*. 2018;71:414–425.
18. Sacks HS, Fain JN. Human epicardial adipose tissue: a review. *Am Heart J*. 2007;153:907–917.
19. Mazurek T, Zhang L, Zalewski A, Mannion JD, Diehl JT, Arafat H, Sarov-Blat L, O'Brien S, Keiper EA, Johnson AG, Martin J, Goldstein BJ, Shi Y. Human epicardial adipose tissue is a source of inflammatory mediators. *Circulation*. 2003;108:2460–2466.
20. Greif M, Becker A, von Ziegler F, Lebherz C, Lehrke M, Broedl UC, Tittus J, Parhofer K, Becker C, Reiser M, Knez A, Leber AW. Pericardial adipose tissue determined by dual source CT is a risk factor for coronary atherosclerosis. *Arterioscler Thromb Vasc Biol*. 2009;29:781–786.
21. Shimabukuro M, Hirata Y, Tabata M, Dagvasumberel M, Sato H, Kurobe H, Fukuda D, Soeki T, Kitagawa T, Takanashi S, Sata M. Epicardial adipose tissue volume and adipocytokine imbalance are strongly linked to human coronary atherosclerosis. *Arterioscler Thromb Vasc Biol*. 2013;33:1077–1084.
22. Furuhashi M, Fuseya T, Murata M, Hoshina K, Ishimura S, Mita T, Watanabe Y, Omori A, Matsumoto M, Sugaya T, Oikawa T, Nishida J, Kokubu N, Tanaka M, Moniwa N, Yoshida H, Sawada N, Shimamoto K, Miura T. Local production of fatty acid-binding protein 4 in epicardial/perivascular fat and macrophages is linked to coronary atherosclerosis. *Arterioscler Thromb Vasc Biol*. 2016;36:825–834.
23. Otsuka F, Yahagi K, Sakakura K, Virmani R. Why is the mammary artery so special and what protects it from atherosclerosis? *Ann Cardiothorac Surg*. 2013;2:519–526.
24. Kitamura S. Physiological and metabolic effects of grafts in coronary artery bypass surgery. *Circ J*. 2011;75:766–772.
25. Nakajima T, Tachibana K, Takagi N, Ito T, Kawaharada N. Histomorphologic superiority of internal thoracic arteries over right gastroepiploic arteries for coronary bypass. *J Thorac Cardiovasc Surg*. 2016;151:1704–1708.

26. Ishimura S, Furuhashi M, Mita T, Fuseya T, Watanabe Y, Hoshina K, Kokubu N, Inoue K, Yoshida H, Miura T. Reduction of endoplasmic reticulum stress inhibits neointima formation after vascular injury. *Sci Rep*. 2014;4:6943.
27. Koyama M, Furuhashi M, Ishimura S, Mita T, Fuseya T, Okazaki Y, Yoshida H, Tsuchihashi K, Miura T. Reduction of endoplasmic reticulum stress by 4-phenylbutyric acid prevents the development of hypoxia-induced pulmonary arterial hypertension. *Am J Physiol Heart Circ Physiol*. 2014;306:H1314–H1323.
28. Cinti S, Mitchell G, Barbatelli G, Murano I, Ceresi E, Faloia E, Wang S, Fortier M, Greenberg AS, Obin MS. Adipocyte death defines macrophage localization and function in adipose tissue of obese mice and humans. *J Lipid Res*. 2005;46:2347–2355.
29. Gesta S, Bluher M, Yamamoto Y, Norris AW, Berndt J, Kralisch S, Boucher J, Lewis C, Kahn CR. Evidence for a role of developmental genes in the origin of obesity and body fat distribution. *Proc Natl Acad Sci U S A*. 2006;103:6676–6681.
30. Tchkonia T, Lenburg M, Thomou T, Giorgadze N, Frampton G, Pirtskhalava T, Cartwright A, Cartwright M, Flanagan J, Karagiannides I, Gerry N, Forse RA, Tchoukalova Y, Jensen MD, Pothoulakis C, Kirkland JL. Identification of depot-specific human fat cell progenitors through distinct expression profiles and developmental gene patterns. *Am J Physiol Endocrinol Metab*. 2007;292:E298–E307.
31. Chatterjee TK, Stoll LL, Denning GM, Harrelson A, Blomkalns AL, Idelman G, Rothenberg FG, Neltner B, Romig-Martin SA, Dickson EW, Rudich S, Weintraub NL. Proinflammatory phenotype of perivascular adipocytes: influence of high-fat feeding. *Circ Res*. 2009;104:541–549.
32. Ho E, Shimada Y. Epicardial covering over myocardial wall in the chicken embryo as seen with the scanning electron microscope. *Dev Biol*. 1978;66:579–585.
33. Rittig K, Dolderer JH, Balletshofer B, Machann J, Schick F, Meile T, Kuper M, Stock UA, Staiger H, Machicao F, Schaller HE, Konigsrainer A, Haring HU, Siegel-Axel DI. The secretion pattern of perivascular fat cells is different from that of subcutaneous and visceral fat cells. *Diabetologia*. 2012;55:1514–1525.
34. Sims FH. A comparison of coronary and internal mammary arteries and implications of the results in the etiology of arteriosclerosis. *Am Heart J*. 1983;105:560–566.
35. van Son JA, Smedts F, Vincent JG, van Lier HJ, Kubat K. Comparative anatomic studies of various arterial conduits for myocardial revascularization. *J Thorac Cardiovasc Surg*. 1990;99:703–707.
36. Ishii T, Asuwa N, Masuda S, Ishikawa Y. The effects of a myocardial bridge on coronary atherosclerosis and ischaemia. *J Pathol*. 1998;185:4–9.
37. Prati F, Arbustini E, Labellarte A, Sommariva L, Pawlowski T, Manzoli A, Pagano A, Motolese M, Boccanelli A. Eccentric atherosclerotic plaques with positive remodelling have a pericardial distribution: a permissive role of epicardial fat? A three-dimensional intravascular ultrasound study of left anterior descending artery lesions. *Eur Heart J*. 2003;24:329–336.
38. Faight E, Verdelis K, Ahearn JM, Shields KJ. 3D MicroCT spatial and temporal characterization of thoracic aorta perivascular adipose tissue and plaque volumes in the ApoE-/- mouse model. *Adipocyte*. 2018;7:156–165.
39. Xiong W, Zhao X, Villacorta L, Rom O, Garcia-Barrio MT, Guo Y, Fan Y, Zhu T, Zhang J, Zeng R, Chen YE, Jiang Z, Chang L. Brown adipocyte-specific ppargamma (peroxisome proliferator-activated receptor gamma) deletion impairs perivascular adipose tissue development and enhances atherosclerosis in mice. *Arterioscler Thromb Vasc Biol*. 2018;38:1738–1747.
40. Vela D, Buja LM, Madjid M, Burke A, Naghavi M, Willerson JT, Casscells SW, Litovsky S. The role of periadventitial fat in atherosclerosis. *Arch Pathol Lab Med*. 2007;131:481–487.
41. Hu D, Mohanta SK, Yin C, Peng L, Ma Z, Srikakulapu P, Grassia G, MacRitchie N, Dever G, Gordon P, Burton FL, Ialenti A, Sabir SR, McInnes IB, Brewer JM, Garside P, Weber C, Lehmann T, Teupser D, Habenicht L, Beer M, Grabner R, Maffia P, Weih F, Habenicht AJ. Artery tertiary lymphoid organs control aorta immunity and protect against atherosclerosis via vascular smooth muscle cell lymphotoxin beta receptors. *Immunity*. 2015;42:1100–1115.
42. Cybularz M, Langbein H, Zatschler B, Brunssen C, Deussen A, Matschke K, Morawietz H. Endothelial function and gene expression in perivascular adipose tissue from internal mammary arteries of obese patients with coronary artery disease. *Atheroscler Suppl*. 2017;30:149–158.
43. Fuseya T, Furuhashi M, Matsumoto M, Watanabe Y, Hoshina K, Mita T, Ishimura S, Tanaka M, Miura T. Ectopic fatty acid-binding protein 4 expression in the vascular endothelium is involved in neointima formation after vascular injury. *J Am Heart Assoc*. 2017;6:e006377. DOI: 10.1161/JAHA.117.006377.
44. Dashwood MR, Loesch A. Inducible nitric oxide synthase and vein graft performance in patients undergoing coronary artery bypass surgery: physiological or pathophysiological role? *Curr Vasc Pharmacol*. 2014;12:144–151.
45. Khan T, Muise ES, Iyengar P, Wang ZV, Chandalia M, Abate N, Zhang BB, Bonaldo P, Chua S, Scherer PE. Metabolic dysregulation and adipose tissue fibrosis: role of collagen VI. *Mol Cell Biol*. 2009;29:1575–1591.
46. Divoux A, Tordjman J, Lacasa D, Veyrie N, Hugol D, Aissat A, Basdevant A, Guerre-Millo M, Poitou C, Zucker JD, Bedossa P, Clement K. Fibrosis in human adipose tissue: composition, distribution, and link with lipid metabolism and fat mass loss. *Diabetes*. 2010;59:2817–2825.
47. Ichioka M, Suganami T, Tsuda N, Shirakawa I, Hirata Y, Satoh-Asahara N, Shimoda Y, Tanaka M, Kim-Saijo M, Miyamoto Y, Kamei Y, Sata M, Ogawa Y. Increased expression of macrophage-inducible c-type lectin in adipose tissue of obese mice and humans. *Diabetes*. 2011;60:819–826.
48. Tanaka M, Ikeda K, Suganami T, Komiya C, Ochi K, Shirakawa I, Hamaguchi M, Nishimura S, Manabe I, Matsuda T, Kimura K, Inoue H, Inagaki Y, Aoe S, Yamasaki S, Ogawa Y. Macrophage-inducible c-type lectin underlies obesity-induced adipose tissue fibrosis. *Nat Commun*. 2014;5:4982.
49. Drosos I, Chalikias G, Pavlaki M, Kareli D, Epitropou G, Bougioukas G, Mikroulis D, Konstantinou F, Giatromanolaki A, Ritis K, Munzel T, Tziakas D, Konstantinides S, Schafer K. Differences between perivascular adipose tissue surrounding the heart and the internal mammary artery: possible role for the leptin-inflammation-fibrosis-hypoxia axis. *Clin Res Cardiol*. 2016;105:887–900.
50. Chatterjee TK, Aronow BJ, Tong WS, Manka D, Tang Y, Bogdanov VY, Unruh D, Blomkalns AL, Piegore MG Jr, Weintraub DS, Rudich SM, Kuhel DG, Hui DY, Weintraub NL. Human coronary artery perivascular adipocytes overexpress genes responsible for regulating vascular morphology, inflammation, and hemostasis. *Physiol Genomics*. 2013;45:697–709.
51. Cao Y. Angiogenesis modulates adipogenesis and obesity. *J Clin Invest*. 2007;117:2362–2368.